Applied Catalysis A: General 433–434 (2012) 96–108

Contents lists available at SciVerse ScienceDirect

Applied Catalysis A: General

journal homepage: www.elsevier.com/locate/apcata

# A kinetics study for the oxidative coupling of methane on a $Mn/Na_2WO_4/SiO_2$ catalyst

T.P. Tiemersma, M.J. Tuinier, F. Gallucci, J.A.M. Kuipers, M. van Sint Annaland *

*Multiphase Reactors Group, Department of Chemical Engineering and Chemistry, Eindhoven University of Technology, P.O. Box 513, 5600 MB, Eindhoven, The Netherlands*

ARTICLE INFO

*Article history:*
Received 12 March 2012
Received in revised form 3 May 2012
Accepted 8 May 2012
Available online 17 May 2012

*Keywords:*
Methane oxidative coupling
Catalysis
Kinetics
$Mn/Na_2WO_4/SiO_2$

ABSTRACT

This paper presents an experimental kinetic study for the oxidative coupling of methane (OCM) over a $Mn/Na_2WO_4/SiO_2$ catalyst prepared by incipient wetness impregnation. Because the catalyst is a reducible metal oxide, the stability of the catalyst has been assessed by Thermo Gravimetric Analysis (TGA). These experiments show that the catalyst has to be pre-treated with oxygen in order to obtain high $C_2$ selectivity (around 85%) and that a low oxygen partial pressure during the OCM reactions is already sufficient to maintain the catalyst stable in the oxidized state.

The catalyst has subsequently been tested in a micro-catalytic fixed bed reactor. The overall reaction orders and rate constants of the primary reactions were determined by measuring the intrinsic reaction rates at different methane and oxygen inlet concentrations. It was found that the reaction order in oxygen for the coupling reaction is 0.38, while the reaction order in oxygen for ethylene oxidation approaches unity, indicating that low oxygen concentration levels are beneficial for obtaining a high $C_2$ selectivity (up to 80–90%). Such a low oxygen concentration can be obtained with distributive feeding in a membrane reactor.

Based on the experiments and least-squares minimization, a simplified reaction mechanism is proposed, where the dependency of the ethane (coupling) and carbon dioxide (oxidation) production rates and the secondary ethylene production and $C_2$ oxidation rates can be described with power-law type reaction rate expressions.



## 1. Introduction

The oxidative coupling of methane (OCM) is a widely investigated direct route for ethylene production through methane partial oxidation. The reaction involved in OCM carried out at temperatures higher than 750 °C are the following:

$$2CH_4 + O_2 \rightarrow C_2H_4 + 2H_2O \quad \Delta H^\circ_{298} = -141\ \mathrm{kJ/mol_{CH_4}} \qquad \text{(i)}$$

$$CH_4 + 2O_2 \rightarrow CO_2 + 2H_2O \quad \Delta H^\circ_{298} = -803\ \mathrm{kJ/mol_{CH_4}} \qquad \text{(ii)}$$

$$C_2H_4 + 3O_2 \rightarrow 2CO_2 + 2H_2O \quad \Delta H^\circ_{298} = -1323\ \mathrm{kJ/mol_{C_2H_4}} \qquad \text{(iii)}$$

The industrial exploitation of such a reaction system is hindered by the low yield typical of this conversion-selectivity problem: high $CH_4$ conversions (i.e. feeding a relatively large amount of $O_2$) are associated with relatively poor product selectivity with a large yield of undesired combustion products like $CO_x$. In addition, the highly reactive intermediate $C_2H_4$ may easily react to the unwanted and thermodynamically favored oxidation products at too high $O_2$ concentrations.

Despite the difficulties in achieving higher yields, this reaction system has always been considered very promising by both industries and research institutions. A total yield higher than 35–40% would already make this system economically feasible. For this reason, since 1980's, many groups investigated the OCM [1,2], mainly focusing on different catalytic materials.

The actual trend in chemical reaction engineering on OCM reaction is towards the development of novel reactor concepts with distributed feeding of oxygen (e.g. with membrane reactors) in order to keep a low concentration of oxygen along the reactor and thus improving the product yield. The design and optimization of such reactors require the development of adequate kinetic models for catalysts operated at high temperatures and low oxygen concentrations.

A widely investigated catalyst for OCM is Li/MgO [3], which is already active and selective at reaction temperatures of 750 °C but is inherently unstable because of the loss of active components.

Usually the research is limited to study the catalyst performance and the determination of a reaction mechanism, however, for reactor modeling and design of a new process involving oxidative coupling of methane, possibly combined with steam reforming, and carried out in membrane reactors an accurate description of the most important reaction rates is required. A quantitative

* Corresponding author. Tel.: +31 40 247 2241; fax: +31 40 247 5833.
*E-mail address:* M.v.SintAnnaland@tue.nl (M.v.S. Annaland).

0926-860X/$ – see front matter © 2012 Elsevier B.V. All rights reserved.
http://dx.doi.org/10.1016/j.apcata.2012.05.002

description of the reaction rates of the most important reactions on a $Mn/WO_4/SiO_2$ catalyst by means of a relatively straightforward kinetic study is the objective of the research described in this paper. A simplified kinetic model is presented, describing the rates of the primary and secondary reactions prevailing during the oxidative coupling of methane over a $Mn/Na_2WO_4/SiO_2$ catalyst. The primary reaction rates were measured in a micro-catalytic fixed bed reactor under differential operating conditions, while the secondary reaction rate constants were derived from a kinetic study by Takanabe and Iglesia [4] in which the first order rate constants were determined by means of isotopic labeling of $CH_4$, $C_2H_4$ and $C_2H_6$.

The obtained reaction rates were described via conventional power-law reaction rate expressions.

This paper starts with a short review of the available catalysts for oxidative coupling and two promising catalysts are discussed in more detail. The preparation of the best performing catalyst, the experimental setup and the procedures followed during the experimental program are described. The composition of the selected catalyst is compared with available data from the literature by analyzing the elements in a small amount of catalyst via X-ray fluorescence (XRF) spectroscopy. Subsequently, it was shown that the (redox) catalyst remains in the oxided state and the percentage of the oxides on the catalyst that can be reduced is measured by means of thermogravimetric analysis. Finally, the homogeneous reaction rates (mostly occuring in the pre- and post-catalytic sections) and the catalytic reaction rates during the oxidative coupling were determined in a micro-catalytic fixed bed reactor by investigating the dependency of the conversion rates on the partial pressures of methane, oxygen, ethylene and ethane. The reaction rates of the relevant reactions are described using power-law reaction rate expressions in a simplified kinetic model.

### 1.1. Review on OCM catalysts

A large number of unsupported and supported catalysts, mostly elements from Group I to II of the Periodic Table, was developed and tested for their catalytic activity and stability for OCM. It has been indicated that for alkaline earth metal (e.g. Mg, Ca, Sr) and promoted rare earth (e.g. La, Ce, Nd) oxide catalysts the performance can be modified by adding an alkaline earth promoter [5].

Unsupported catalysts with a better activity and selectivity are for example lanthanide oxides $Nd_2O_3$, $Eu_2O_3$ and $La_2O_3$ [6], where the strong basic sites of e.g. La and Nd oxides result in improved catalytic activity. The activity can be increased by doping with Ce or Nd, addition of 10 wt% ceria showed an increase in the $C_2$ yield to 20–22% [7]. The Sr-promoted $La_2O_3$ showed however the best performance according to Choudhary and Uphade [5].

The $C_2$ yield (15–20%) of these catalysts is acceptable, however, unsupported catalysts are less applicable in industrial environment due to their weak mechanical strength and limited reaction rate per unit catalyst volume.

Numerous studies have been performed to determine which is the best catalyst/support combination for OCM and some of the highlights have been listed in Table 1, for several inlet $CH_4/O_2$ concentrations.

The $C_2$ yield that can be achieved with supported catalysts varies between 12 and 21%, at relatively similar temperatures. However, the catalytic activity should also be taken into account (represented by the $CH_4$ reaction rate), because it determines the required reactor volume and the volumetric heat generation. For example, the Li/MgO catalyst has a relatively low activity (also at higher GHSV), but a very acceptable $C_2$ yield of 19%.

Next to selectivity and activity, another important issue for OCM catalysts is the long-term stability; because of the high operating temperature and the prevailing exothermic reactions, the active catalytic components tend to migrate or even evaporate from the catalytic surface leading to deactivation of the catalyst. For catalysts, such as the Li/MgO catalyst, the high mobility of Li limits the lifetime and thus the industrial applicability.

The problem can be partially solved by using excess catalyst, thereby decreasing the utilization of the catalytic bed, and by selecting a catalyst with high activity such as $La_2O_3$. If the catalyst gradually deactivates, the remaining catalyst will be used until the overall activity becomes unacceptable, however at the expense of throughput. Another method is to apply a catalyst with better stability but with lower activity, such as the $Mn/Na_2WO_4$ catalyst. The properties and performance of these two catalysts are discussed in somewhat more detail below.

#### 1.1.1. The $La_2CO_3$/CaO catalyst

In the literature it is found that if OCM catalysts are promoted by lanthanoids or alkali metals, additional activity and selectivity is observed during kinetic experiments [5]. A catalyst showing a great thermal and hydrothermal stability is the $La_2CO_3$ catalyst which was tested on oxidative coupling activity for periods up to 500 h on stream [9].

High $C_2$ yields were experimentally observed with the use of rare earth oxides promoted with alkaline earth metals as catalyst. As shown in Table 1, the Sr-promoted $La_2O_3$ with a Sr/La ratio of 0.1 showed good results at an $CH_4/O_2$ inlet ratio of 4.0 and a temperature of 800 °C, at which a $CH_4$ conversion of approximately 28–29% and a yield around 18% could be obtained [5].

The support of this catalyst is equally important, because it partially determines the catalytic performance because of its surface basicity, larger surface area and lower cost. In addition, when catalysts are applied in industrial scale reactors the support provides mechanical strength (crushing strength) and a lower pressure drop across the catalyst bed. The activity and selectivity of Li/MgO catalysts were drastically reduced when they were supported on different catalyst carriers due to formation of metal oxides containing Li and Mg, because the basicity of the active sites was strongly influenced by the origin of the support and the deactivation because of chemical interaction between support and catalyst. However, the most active catalysts reported for oxidative coupling of methane is the $La_2O_3$ catalyst supported on CaO, which has been proposed by a.o. Becker and Baerns [17].

#### 1.1.2. The $Mn/Na_2WO_4/SiO_2$ catalyst

With most catalysts, the overall $C_2$ product yield obtained in single pass operation mode does not exceed 25–30%, which is the generally considered lower limit for commercialization of OCM [5,18,19].

In the 1990s, however, an active and stable catalyst has been developed by Fang et al. [20], who identified sodium-promoted manganese oxides as promising catalysts for the oxidative coupling of methane.

Catalysts based on manganese oxides were already suggested as good OCM catalysts by Sofranko et al. [21], who measured methane conversion rates over various transition metal oxides in a redox cyclic mode of operation. From the investigated transition metal oxides, only manganese and tin oxides remained stable, while an overall $C_2$ selectivity of more than 75% was achieved on the more stable and less volatile manganese oxides supported on $SiO_2$ at temperatures around 800 °C [21,22].

By addition of alkali metals or alkaline earth metals, the surface basicity and the interaction between the alkali metal ions and the manganese oxides leads to suppression of carbon oxide formation [23]. This method was further developed and used by Fang et al. [20] into a catalyst containing 2 wt% Mn/5 wt% $Na_2WO_4$ supported on $SiO_2$, which appeared to have a much higher stability probably thanks to by the presence of tungsten.

**Table 1**
Reactivity and performance of supported OCM catalysts.[a]

| Catalyst | $CH_4/O_2$ (−) | $T$ (°C) | $\xi_{CH_4}$ (%) | $S_{C_2+}$ (%) | $Y_{C_2+}$ (%) | $r_{CH_4}$ (μmol/(g s)) | $m_{cat}$ (g) | GHSV (ml/g/h) | Reference |
|---|---|---|---|---|---|---|---|---|---|
| *Unsupported* | | | | | | | | | |
| La/CaO | 4 | 800 | 28 | 56 | 16 | | 1 | | [7] |
| Ce/MgO | 4 | 800 | 28 | 50 | 14 | | 1 | | [7] |
| $Sr/La_2O_3$ | 4 | 800 | 29 | 59 | 17 | | 1 | | [8] |
| $La_2O_3$ | 5.4 | 800 | 24.0 | 65.0 | 15.6 | 49.6 | 0.3 | 19,977 | [9] |
| *Supported* | | | | | | | | | |
| Li/MgO | 2 | 750 | 37.8 | 50.3 | 19.0 | 0.268 | 4 | 747 | [2] |
| $Pb/SiO_2$ | 6 | 750 | 13.0 | 58.2 | 7.6 | 57.2 | 0.1 | 119,880 | [10] |
| $Mn/Na_2WO_4/MgO$ | 7.4 | 800 | 20.0 | 80.0 | 16.0 | 6.9 | 2.1 | 3212 | [11] |
| Li/Sn/MgO | 9.6 | 680 | 14.3 | 84.0 | 12.0 | 18.7 | 0.75 | 15,984 | [3] |
| *The $Mn/Na_2WO_4$ catalyst* | | | | | | | | | |
| 1.9% Mn/5% $Na_2WO_4$ | 4.5 | 850 | 33 | 80 | 26 | 2.8 | 0.40 | 2700 | [12] |
| 2% Mn/x% Na/3% $WO_4$ | 3.0 | 800 | 33 | 59 | 19 | 2.1 | 0.10 | 70,560 | [13] |
| 2% $Mn_2O_3$/5% $Na_2WO_4$ | 4.0 | 780 | 33 | 37 | 12 | 6.3 | 0.40 | 196,110 | [14] |
| 2% Mn/5% $Na_2WO_4$ | 7.4 | 800 | 20 | 80 | 16 | 2.8 | 0.51 | 12,917 | [15] |
| 2% Mn/5% $Na_2WO_4$ | 3.0 | 800 | 36.8 | 64.9 | | | | | [16] |
| $Mn/Na_2WO_4/SiO_2$ | 4 | 820 | 30 | 68 | 21 | | 0.2 | 30,000 | [11] |

[a] $CH_4/O_2$ ratio = 2–10, $p$ = 1 bar.

Further optimization of a *x*%Na-3.1%W-2%Mn/$SiO_2$ catalyst (*x* varying from 0 to 7.8 wt%) indicates that a good catalytic performance can only be obtained if all 3 metals of this trimetallic system are present at the catalyst surface [13].

For example, there is an optimum Na-concentration at the catalyst surface, which influences the near-surface composition of W and Mn. The addition of Na decreases the CO selectivity; with sodium free catalyst a CO selectivity of approximately 61% is realized but this value decreases to about 13% on a catalyst containing 0.8 wt% Na.

A strong correlation exists between the surface Mn concentration and the catalyst performance, hence, a too high Na load will cause enrichment of Na near the surface resulting in a decrease of the surface Mn concentration, directly affecting the $CH_4$ conversion and $C_2$ selectivity, see [13]. By doping the catalyst with $SnO_2$, a significant increase of the $CH_4$ conversion up to 33% and a corresponding $C_2^+$ selectivity of approximately 73% can be achieved. Cofeeding oxygen and methane without diluent at elevated pressure (6–10 bar), $CH_4/O_2$ ratio of 6 and high GHSV resulted in much higher $C_2^+$ selectivity mainly because of the production of $C_3$ (30%) and $C_4$ (4%) components, which is remarkably higher than found with other investigated catalysts [14]. The reason for the remarkable increase in conversion and selectivity is thought to be the improvement in $O_2$ storage capacity due to the addition of $SnO_2$, while the migration of catalytic species to the catalyst surface is also enhanced [14]. This behavior was also observed with the addition of $Na_2WO_4$ to a catalyst consisting of $Mn/SiO_2$ [13].

The stability of the $Mn/Na_2WO_4$ catalyst on $SiO_2$ and MgO was investigated in the cofeed and pulsed feed mode in a fixed bed microreactor (alumina tubes) at temperatures varying from 750 to 800 °C and $CH_4/O_2$ ratios between 5 and 10 (integral operation). During an on-stream time of at least 30 h, the $CH_4$ conversion and $C_2$ selectivity could be maintained at constant values of respectively 20% and 80%, with both the $Mn/Na_2WO_4/SiO_2$ and the $Mn/Na_2WO_4/MgO$ catalyst [24].

The activity of the MgO based catalyst could however not be retained because of a significant decrease in surface area during the operation. The $SiO_2$ based catalyst appeared to be stable under integral and differential conditions, showing that $O_2$ deficiency does not play a role in the deactivation. In contrast to other researchers who all conclude that the catalyst is highly stable during very long operating time (>500 h), Pak and Lunsford [25] concluded that the $Mn/Na_2WO_4/SiO_2$ catalyst gradually deactivates over time, but that this effect is partially compensated or masked by the observed hot spots in the reactor, which they confirmed by investigating the temperature profiles along the axial reactor coordinate.

Experimental results performed by different research groups showed that the catalyst shows excellent overall $C_2$ selectivity (80%) at moderate $CH_4$ conversions (20–25%), especially under oxygen limiting conditions [24]. Long-term experiments under OCM conditions also demonstrated that the initial activity could be retained for periods up to 97 h in a small fixed bed reactor [25] and even up to 450 h in a fluidized bed reactor [26].

For this reason the $Mn/Na_2WO_4/SiO_2$ catalyst is one of the best and most promising catalysts available for the oxidative coupling of methane, especially in packed bed membrane reactors.

Another advantage is the easy preparation of this catalyst. The $Mn/Na_2WO_4/SiO_2$ catalyst can be very easily prepared from readily available chemicals. The most common way to produce $Mn/Na_2WO_4$ catalyst on $SiO_2$ is incipient wetness impregnation with aqueous solutions of $Mn(NO_3)_2$ and $Na_2WO_4$ at 85–90 °C [11–13,27,28] followed by drying in air or $O_2$ at 80–130 °C.

Although 50–90 °C is the most often used impregnation temperature, some researchers also appear to carry out this step at room temperature [12]. Calcination of the catalyst is carried out under flowing air/oxygen at temperatures in the range of 800–900 °C. Chou et al. [14] applied equal volume impregnation at 54 °C and subsequent impregnation with toluene solutions containing 5% di-n-butyltin dilaurate to obtain ($SnO_2$ doped) $Mn_2O_3$/5% $Na_2WO_4/SiO_2$. The composition of the catalyst was optimized to a large extent by Fang et al. [20] and it was found that a catalyst with a loading of 2 wt% Mn and 5 wt% $Na_2WO_4$ results in high selectivity and methane conversion. This was confirmed by other researchers, who determined an optimal catalyst composition of 0.8 wt% Na/3.1 wt% W/1.2 wt% Mn on $SiO_2$ [13,18,20].

### *1.2. Reaction mechanisms proposed in literature and influence of operating conditions*

It is generally accepted that the heterogeneously catalytized oxidative coupling reaction involves the abstraction of a H-atom from methane by the adsorbed $O_2$ species, leading to the formation of methyl radicals at the catalyst surface. The generated intermediate methyl radicals then react further to form the primary reaction products, ethane and carbon oxides in the gas phase via branched chain reactions in the pores of the catalyst and in the void space between the catalyst pellets [29]. The reaction mechanism of OCM on $Mn/Na_2WO_4/SiO_2$ appears to be similar to that of other OCM catalysts [15].

The reaction network is complex involving many heterogeneous surface and homogeneous gas phase reactions. Many kinetic models have been developed with varying complexity, depending on whether surface and gas phase reactions have been accounted for separately [4,8,29,30].

In this study, where the quantitative description of the consumption and production rates of the main gas phase components is the primary objective, some relatively unimportant reactions were ignored and other reactions lumped together, so that the reaction rate expressions are simplified and the kinetic model is determined based on the most important primary and secondary reactions.

*1.2.1. Primary reactions*

During the initial stage of the reaction, the methyl radicals are coupled near the catalytic surface to form $C_2H_6$, CO and/or $CO_2$ [5,8,31].

$$CH_4 + (1/2)O_2 \rightarrow C_2H_6 + H_2O \quad \Delta H^\circ_{298} = -88.3\,\text{kJ/mol}_{CH_4} \quad (1)$$

$$CH_4 + 2O_2 \rightarrow CO_2 + 2H_2O \quad \Delta H^\circ_{298} = -802\,\text{kJ/mol}_{CH_4} \quad (2)$$

$$CH_4 + H_2O \Leftrightarrow CO + 3H_2 \quad \Delta H^\circ_{298} = -200\,\text{kJ/mol}_{CH_4} \quad (3)$$

$$CH_4 + O_2 \rightarrow CO + H_2O{+}H_2 \quad \Delta H^\circ_{298} = -277.8\,\text{kJ/mol}_{CH_4} \quad (4)$$

At differential operating conditions, ethylene is only formed in very small quantities as a primary product, whereas at higher $CH_4$ conversion the bulk of $C_2H_4$ is formed via either oxidative or thermal dehydrogenation reactions [15].

Carbon dioxide is considered as both a primary and secondary reaction product, and it was found that the origin of $CO_2$ of the primary reaction is the combustion of methane. A simplified scheme of the reaction network was presented (in slightly different forms) (e.g. [4,8]).

*1.2.2. Secondary reactions*

A good OCM catalyst should generate sufficient methyl radicals (activity) and take care that these radicals couple to form $C_2H_6$ before unselective or secondary reactions take place. Increase in the rate of secondary reactions, which occurs at increasing $O_2$ and $C_2$ concentration levels, will inevitably lead to loss of selectivity and additional heat production [32].

$$C_2H_6 + (1/2)O_2 \rightarrow C_2H_4 + H_2O \quad \Delta H^\circ_{298} = -105.5\,\text{kJ/mol}_{C_2H_6} \quad (5)$$

$$C_2H_6 \rightarrow C_2H_4 + H_2 \quad \Delta H^\circ_{298} = +136\,\text{kJ/mol}_{C_2H_6} \quad (6)$$

$$C_2H_6 + (7/2)O_2 \rightarrow 2CO_2 + 3H_2O \quad \Delta H^\circ_{298} = -1428.7\,\text{kJ/mol}_{C_2H_6} \quad (7)$$

$$C_2H_6 + (5/2)O_2 \rightarrow 2CO_2 + 3H_2O \quad \Delta H^\circ_{298} = -757\,\text{kJ/mol}_{C_2H_6} \quad (8)$$

$$C_2H_4 + 3O_2 \rightarrow 2CO_2 + 2H_2O \quad \Delta H^\circ_{298} = -1323.2\,\text{kJ/mol}_{C_2H_4} \quad (9)$$

$$C_2H_4 + 2O_2 \rightarrow 2CO + 2H_2O \quad \Delta H^\circ_{298} = -757.2\,\text{kJ/mol}_{C_2H_4} \quad (10)$$

$$CO + H_2O \Leftrightarrow CO_2 + H_2 \quad \Delta H^\circ_{298} = -41\,\text{kJ/mol}_{CO} \quad (11)$$

$$CO + (1/2)O_2 \rightarrow CO_2 \quad \Delta H^\circ_{298} = -283\,\text{kJ/mol}_{CO} \quad (12)$$

$$H_2 + (1/2)O_2 \rightarrow H_2O \quad \Delta H^\circ_{298} = -241\,\text{kJ/mol}_{H_2} \quad (13)$$

Ethylene is considered as a secondary product formed by oxidative dehydrogenation or thermal cracking of ethane, which was demonstrated by Pak et al. [15] who compared the $C_2H_4$ formation rate under differential and integral conditions. The subsequent oxidation reactions will only be prominent if the concentration of $C_2H_4$ is sufficiently high, which is typically downstream in the reactor.

The first reaction leading to $C_2H_4$ formation is the oxidative dehydrogenation of ethane (reaction (5)), while the second reaction is the thermal dehydrogenation of ethane (reaction (6)). It was found that co-feeding ethane with methane and oxygen to a reactor in the absence of a catalyst leads to a greatly increased overall conversion, because it led to an increased radical concentration and hence higher branching rates ($C_2H_6$ has a lower C—H bond energy than $CH_4$). Although this beneficial effect disappears when the ethane-to-methane inlet ratio exceeds 0.04 [33], it increases the opportunity of using natural gas as a carbon source (well-head quality natural gas typically contains some ethane).

Co-feeding of ethane in the presence of a Sn/Li/MgO catalyst during the OCM reaction resulted in a higher ethylene concentration combined with a lower methane conversion, and measurement of the $^{13}C$ content in both ethylene and ethane confirmed that the main source of ethylene is ethane [32].

Although both CO and $CO_2$ are considered as primary reaction products [34–36], a large part of carbon oxides is also formed via combustion of $C_2H_4$ [25]. However, it was also found during studies into the source of $CO_x$ that at lower temperatures deep oxidation mainly occurs via methane combustion. As the temperature increases, at which OCM is favored, the primary source of $CO_x$ products is predominantly the combustion of ethylene and ethane [32].

*1.2.3. Influence of operating conditions*

The critical parameter which determines the performance of oxidative coupling of methane clearly is the oxygen concentration in the reactor. Because $O_2$ is involved as a surface species, oxygen needs to be present in sufficient amounts to provide a continuous supply of $O_2$ to the OCM reaction on the catalyst surface [15]. The range in which the oxygen inlet concentration can be varied is at least limited by 2 constraints. First, because of the highly exothermic reactions a relatively high methane-to-oxygen ratio is required to overcome heat removal problems and to keep the (local) methane conversion sufficiently low. When pre-mixed feed is applied, the lower a $CH_4/O_2$ ratio is determined by the upper flammability limit of methane–oxygen mixtures, which amounts approximately 60–65 mol% $CH_4$ at atmospheric conditions [34].

Distributed feed of $O_2$ can be applied to have sufficiently low local $O_2$ concentrations to overcome too high reactor temperatures and to remain below the flammability limits.

Because $O_2$ is a surface species, and many OCM catalysts are redox type catalysts, the performance of the OCM process with premixed feed of oxygen and methane was compared with operation in the cyclic mode, in which oxygen and methane are sequentially fed to the reactor (avoiding direct contact between gaseous oxygen and methane). During this reaction, lattice oxygen is the main reactant in the coupling reaction instead of gaseous/molecular $O_2$.

It was shown that with longer reduction time ($CH_4$ cycle) the overall time-averaged methane conversion drops significantly while the $C_2$ selectivity increases at temperatures varying from 800 to 850 °C. Because of the limited run time lengths of only 0 to 5 min, the overall yield per time is low. In large (industrial) reactors the presence of gaseous $O_2$ is preferred for maximizing conversion and selectivity [22].

The oxygen concentration has a large influence on the $C_2$ selectivity that can be obtained. The decreased $C_2$ selectivity at high $O_2$ concentrations was for observed on any OCM catalyst, see e.g. [3,15,31].

Because of the lower $O_2$ reaction order for the OCM reaction ($C_2H_6$ production), a high $C_2$ selectivity will be achieved at lower $O_2$ levels at the expense of a lower methane conversion at increasing methane-to-oxygen ratio. This does not necessarily mean that the highest $C_2$ yield is also obtained at a low $O_2$ concentration, because there is a threshold between higher methane conversion and higher $C_2$ selectivity.

Using a too low $O_2$ concentration might however lead to extinction of the reaction, as observed by Sofranko et al. [21] who identified that molecular oxygen should always be present in order to achieve sufficient $CH_4$ conversion (15–20%) at high $C_2$ selectivity

(80–90%). Hence, there will be an optimum $O_2$ concentration for maximum $C_2$ yield.

#### 1.2.4. Effect of reactor pressure

The effect of the total pressure on the reaction rates of OCM was investigated over a wide range varying from 100 to 800 kPa. For a catalyst with a relatively low catalytic activity, such as the $Mn/Na_2WO_4/SiO_2$ catalyst, and especially at higher pressures (>600 kPa) the influence of gas phase reactions becomes important. At high pressure and high residence time, it was found that the only significant effect of the catalyst is the conversion of CO into $CO_2$ and the selectivity towards $C_2$ products decreases [34,37]. In addition, gas-phase reactions in the pre and post catalytic space can become dominant at pressures above 1000 kPa, which can lead to uncontrollable selectivity. The contribution of the pre- and post catalytic volume to the OCM process can be minimized by reduction of the available volume and the temperature in this zone (by introducing e.g. steep temperature gradients).

The effect of elevated reactor pressures on the catalytic reaction rates was investigated with a $SiO_2$ based catalyst at a constant space velocity and a $CH_4/O_2$ ratio of 10. The influence on $CH_4$ conversion and $C_2$ selectivity was very small, which indicated that the productivity of $C_2$ hydrocarbons per unit mass of catalyst is higher, because of the higher mass velocity at elevated pressure [11].

Similar observations were also reported by other researchers; however, they also discussed the thermal effects which accompany the coupling and combustion reactions. Although only 20–40 mg catalyst was used at differential operating conditions, a temperature increase of almost 82 °C over a length of approximately 6 mm was measured during experiments for both MgO and $SiO_2$ based catalysts in the unsteady state; the large temperature gradient can be partially attributed to the high initial activity of the catalyst [11,25].

#### 1.2.5. Effect of reactor temperature

The influence of the operating temperature on oxidative coupling is significant, although bound to maximum temperatures because of catalyst stability and selectivity problems. Because the activation energy of the selective coupling reaction is typically higher than for the primary reactions, the selective reaction is much more sensitive to temperature variations. Therefore, a high temperature is desired for maximum reaction rate. Although at reactor temperatures in the range from 675 to 750 °C the selectivity towards $C_2$ products keeps increasing with rising temperature, already at 750 °C the contribution of homogeneous gas-phase reactions can be relatively high.

The gas phase reactions play an important role in oxidative coupling (increase in the yield of $C_2$ products). At temperatures above 825 °C and a pressure of 130 kPa it was found that a $C_2$ yield of 20% could be reached over a Sn/Li/MgO catalyst and on a Li/MgO catalyst; it was concluded that the higher yield is partially achieved due to thermal cracking of ethane to ethylene [3,34]. If the reactor temperature, however, becomes too high, the contribution of non-selective gas-phase reactions becomes important. Moreover, most OCM catalysts deactivate at a faster rate at higher temperatures, which makes it difficult to maintain steady state operation for the endurance of an experiment. Typically the lifetime of a Li/MgO catalyst is limited to 100 h, but this can be enhanced by limiting the reactor temperature [3,31] and doping of the Li/MgO catalyst with e.g. tin. Other catalysts, such as the $Mn/Na_2WO_4$ catalyst, can perform at much higher temperatures (850–900 °C), which allow the use of a higher temperature and simultaneously producing sufficient $C_2$ products.

## 2. Experimental

### 2.1. Catalyst preparation

In this work, the $Mn/Na_2WO_4$ on $SiO_2$ catalyst is prepared by the two-step incipient wetness impregnation using solutions of pure $Mn(NO_3)_2$ and $Na_2WO_4$ obtained from Sigma Aldrich. The carrier is commercially available silica, Sigma Aldrich grade 10181. The impregnated silica is then calcined at 850 or 900 °C in air.

### 2.2. Catalyst characterization

The calcined silica has been characterized by means of XRF analysis. After calcination the catalyst contains approximately 2 wt% Mn and 5 wt% $Na_2WO_4$ (see Table 2).

Before the kinetic experiments were performed, it was verified that the catalyst preparation method is reproducible and that the activity and the selectivity are comparable with results published in literature. With a calcination temperature of 900 °C a $C_2$ yield of 20% could be obtained at a $CH_4$ conversion of 30%, the small obtained differences with the reported literature data can be attributed to the use of air in this work instead of pure oxygen often used in the literature.

The observed reactions rates are very similar to published values (e.g. [11]). During the explorative experiments, however, under differential conditions, at various flow rates and reaction temperatures, it was found that the reaction rates are slowly decreasing with time on stream, which could indicate catalyst deactivation by either migration of active components, sintering of the structure or blocking of the active sites (e.g. by carboneaceous species or reaction products).

The possibility of migration of active components, which increases at higher operating temperatures, was excluded by an experiment where the flow of methane and oxygen to the reactor was switched off (after a short purge with $N_2$), and switched back after a couple of minutes.

If the loss of active components would be the main reason for the decreasing reaction rates, it is expected that reaction rates will be at the same level again after switching back to the reactor mode. However, after switching back to the feed flow the activity was only partially restored, from which it is concluded that migration is not the main mechanism for the decrease in catalytic activity at this short time scale.

Adsorption of species (such as $C_2H_4$ and $C_2H_6$) at the catalyst surface could also be a possibility, although under the applied conditions the formation of carbonaceous species on the catalyst surface is thermodynamically possible and therefore much more likely. When the reactor flow is stopped, the carbonaceous deposits can possibly disappear during the period of no feed flow by reaction with the remaining oxygen. This was verified with Thermal Gravity Analysis (TGA) by switching flow between a methane rich flow (50% $CH_4$/50% $N_2$) and an air flow. During the period of reduction, however, the sample mass decreased to a constant value whereas coke formation would have led to an increase of the sample mass (see Figs. 1 and 2).

**Table 2**
Measured composition of the $Mn/Na_2WO_4/SiO_2$ catalyst by X-ray fluorescence analysis (XRF).

| Analysis | $m_{sample}$ (mg) | Na (wt%) | Mn (wt%) | W (wt%) |
|---|---|---|---|---|
| 1 | 614.9 | 0.95 | 2.47 | 2.78 |
| 2 | 532.7 | 0.95 | 2.49 | 2.80 |
| Average | | 0.95 | 2.48 | 2.79 |

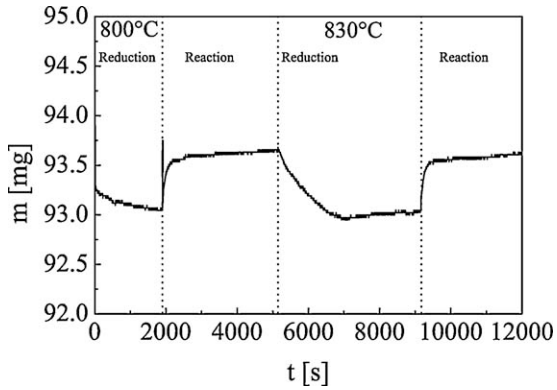


**Fig. 1.** Mass of a $Mn/Na_2WO_4/SiO_2$ sample obtained with Thermal Gravity Analysis (TGA) at different temperatures with a reduction cycle with $H_2$ and oxidation cycle with an OCM reaction mixture of 4% $O_2$, 25% $CH_4$, balance $N_2$.

After oxidation in air, the original sample mass was retained thus there is another mechanism responsible for the changes in the activity.

It was found that after oxidation with air (and a short flush of the reactor with $N_2$), the $C_2$ selectivity was significantly improved from 60% to 70% if a reaction mixture was fed to the sample container. Apparently, the oxidation state of the catalyst is important for the performance of oxidative coupling. Oxidation of the $Mn/Na_2WO_4$ catalyst is possible, Mn for example can exist as Mn, MnO, $Mn_3O_4$ or $MnO_2$ (indeed Mn has been indicated as possible oxygen carrier for chemical looping processes). A possible occurring transition might be the oxidation of MnO to $Mn_3O_4$. XRF measurements have shown that the catalyst contains 2.48 wt% Mn, if this is present as MnO the oxidation of MnO to $Mn_3O_4$ will theoretically result in a mass increase of 0.45 mg. TGA experiments were performed at 800 and 830 °C by first fully reducing a catalyst sample under $H_2$, followed by switching to a feed mixture which equals the feed composition used in the kinetic set-up.

In Fig. 1 it is shown that feeding a reaction mixture to a fully reduced catalyst sample causes the reduced catalyst to increase in weight with 0.54 mg from approximately 93 to 93.5 mg, which is in the same order of magnitude as the theoretical calculation. Furthermore, from the relatively stable operation during OCM it can be concluded that the catalyst remains sufficiently oxidized under reaction conditions to maintain a good OCM performance, which is surprising, because the $CH_4$ concentration is a factor 6 higher than oxygen.

This result is however supported by different TGA experiments, with a mixture containing oxygen fractions of 0.5% and 1%, which are still able to oxidize the catalyst.

It can be concluded that the long time required for steady state is caused by slowly oxidizing the catalyst and this can be resolved by flushing the reactor with air before starting the kinetic experiments.

### 2.3. Procedure for kinetic experiments

The reaction rates of the primary reactions prevailing during OCM over a $Mn/Na_2WO_4/SiO_2$ catalyst were measured under differential conditions. The experimental set-up, contains a feed section, a micro-catalytic fixed bed reactor and an analysis section. In the feed section, the desired feed gas flow rate and composition are controlled by mass flow controllers (Brooks 5850S) for methane, air and nitrogen, as well as ethane or ethylene.

The feed mixture can be sent over a bypass to measure the exact feed composition or fed to the reactor. The reactor is a micro-catalytic fixed bed reactor (ID = 5 mm) made of quartz in which the inlet and outlet temperatures are measured. It is positioned inside a fluidized sand bed oven, resulting in very high external heat exchange and virtual isothermal operation. The feed and product streams are analyzed by online gas chromatography (GC), with a Varian Micro-GC 4900 containing three columns, two 5 Å molsieve columns to separate oxygen, nitrogen, methane, carbon monoxide and hydrogen and a PoraPLOT Q column to separate $H_2O$, $CO_2$, $C_2$ and $C_3$ components. The columns are equipped with thermal conductivity detectors.

Most water is condensed after the reactor, in order to protect the molsieve columns. Nitrogen balance is used to calculate outlet mole fractions and the amount of condensed water is computed from the hydrogen atom balance. Resulting errors in oxygen and carbon atom mass balances are within 1% and in most cases even within 0.5%.

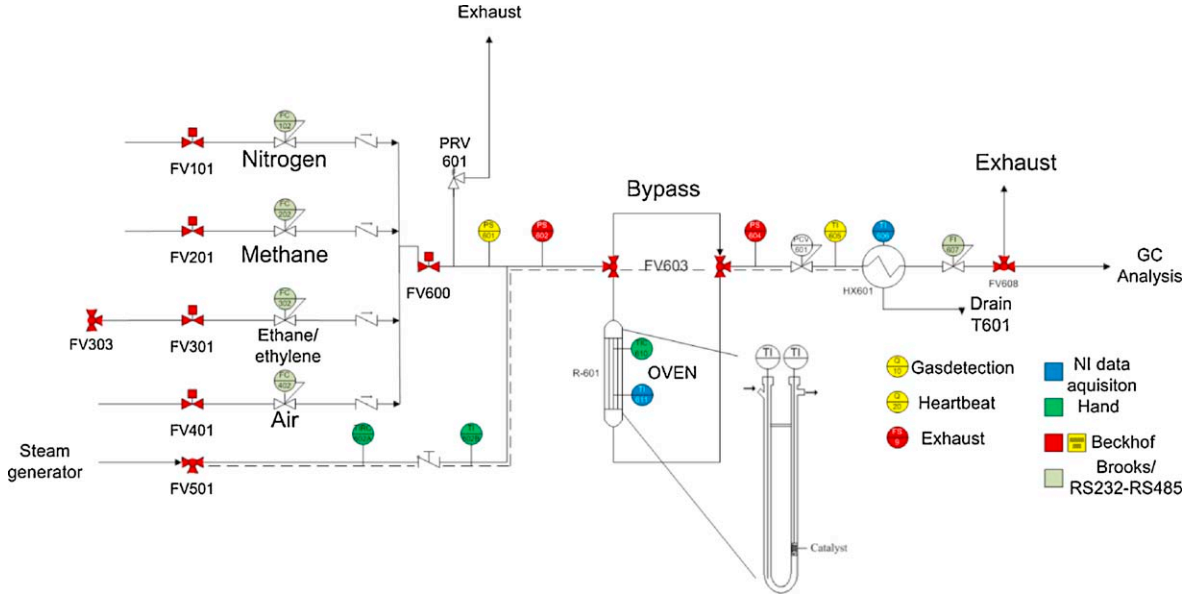


**Fig. 2.** Process flow diagram of the experimental setup with the micro-catalytic fixed bed reactor.

**Table 3**
Diagnostic criteria for checking absence of mass and heat transfer limitations [41,42].

| | | |
|---|---|---|
| Intraparticle | Mass | $\frac{n+1}{2}\frac{R_i\cdot(d_p/6)^2}{D_{eff}\cdot c_i^0} < 0.25$ |
| | Heat | $\frac{\lvert\Delta H\rvert\cdot R_i\cdot d_p^2}{\lambda_s\cdot T_s} < 3\frac{T_s-R_g}{E_a}$ |
| Interphase | Mass | $\frac{c_{bulk}-c_{surface}}{c_{bulk}} < 0.05$ |
| | Heat | $\frac{\lvert\Delta H\rvert\cdot R_i\cdot d_p^2}{\alpha\cdot T} < 0.3\frac{T_s-R_g}{E_a}$ |
| Isothermal | Radial | $\frac{\lvert\Delta H\rvert\cdot R_i\cdot d_p^2}{\lambda_{e,r}\cdot T} < 1.6\frac{T\cdot R_g}{E_a\cdot(1+8\cdot(d_p/d_r\cdot Bi_W))}$ |

### 2.3.1. Absence of mass and heat transfer limitations

For kinetic measurements, it should be ensured that mass and heat transfer limitations are absent so that differential conditions can be attained and that the intrinsic reaction kinetics can be measured. Temperature and concentration gradients can occur inside the catalyst particle, between the particle surface and surrounding gas film as well as between the particles and the bulk gas phase. Several analytical criteria have been reported to check for these limitations, which have been listed in Tables 3 and 4.

It was found that none of these criteria becomes limiting under the conditions investigated, however, care must be taken because the criteria for mass transport limitations usually concern limitations for reactants and products because the catalytic reaction intermediates only exist on the catalytic surface. During high temperature reactions such as oxidative coupling, however, the catalyst produces methyl radicals which react further in the gas phase to ethane or are oxidized to carbon oxides. It has been reported that transport of these radicals could also become rate determining [29]. Therefore absence of mass transfer limitations will also be verified experimentally in this work.

### 2.3.2. Intra-particle limitations

To check for intra-particle limitations, measurements with different particle sizes have been performed. If no limitations occur, the observed reaction rate should be independent of the particle diameter. Catalyst particles of 300–600 μm have been partly crushed and sieved to a fraction of 100–300 μm. Reaction rates were measured for both catalyst fractions.

Fig. 3 shows only slightly reduced reaction rates for the larger particles, so that it can be concluded that intra-particle mass transfer limitations do not play a significant role. Analytical evaluation of the criterion for intra-particle heat transfer already showed that isothermicity inside the catalyst particle is satisfied, therefore it can be concluded that intra-particle limitations are not significant.

### 2.3.3. External limitations

External mass transport occurs in a stagnant layer around the particles through which reactants and products will diffuse. At higher flow rates the thickness of this stagnant film will be reduced and measured reaction rates will be higher if external mass transport limitations will play a role. If no limitations occur, measured rates must be equal for both flow rates at the same gas residence time. External mass transport limitations can be verified experimentally by measuring reaction rates at different flow rates and catalyst amounts, keeping the GHSV (contact time) unchanged. In Fig. 4 the results of four cases are shown.

**Table 4**
Operating conditions used in the kinetic experiments.

| Description | Value | Unit |
|---|---|---|
| Particle size | 0.3–0.5 | mm |
| Temperature | 800–900 | °C |
| Total pressure | 200 | kPa |
| Catalyst | 0.25–0.50 | g |
| $O_2$ partial pressure | 0.7–28.2 | kPa |
| $CH_4$ partial pressure | 9.7–89.6 | kPa |
| Total flow rate | 250 | Nml/min |

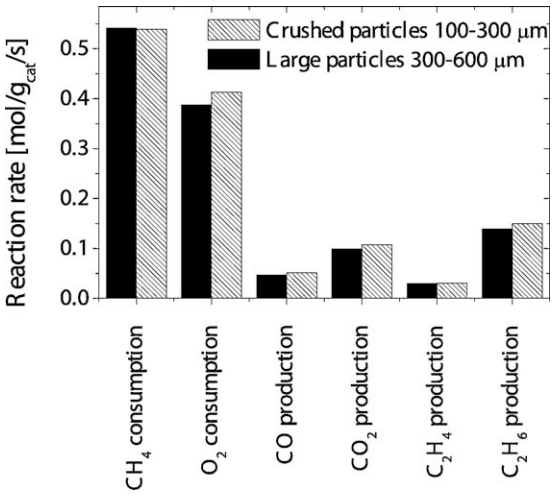


**Fig. 3.** Reaction rates for different catalyst particle sizes ($p_{o_2}$ = 8.1 kPa, $p_{CH_4}$ = 49.6 kPa, $T$ = 800 °C, $p$ = 200 kPa, $\phi_{v,tot}$ = 200 Nml/min, $m_{cat}$ = 0.25 g).

The figure shows slightly lower reaction rates at 500 ml/min (for both amounts of catalyst). This result is remarkable, considering the fact that a higher rate was expected if a transport limitation prevails, because the stagnant film layer thickness should decrease. Therefore it can be concluded that external mass transport limitations do not play a significant role.

The lower reaction rates at higher flow rates can possibly be explained by a reduction of gas phase reactions, as the residence time in pre and post catalytic zones is reduced.

### 2.3.4. Extent of homogeneous reactions

It is expected that without a catalyst present, gas phase reactions will occur due to the high temperatures in the OCM process. This was confirmed with experiments at different temperatures, where the contribution of gas phase reactions was measured in an empty tube reactor. Two reactor materials have been used; stainless steel and quartz. With the stainless steel tube unacceptably high $CH_4$ and $O_2$ conversions of 54% and 100% respectively at 810 °C were found and significant amounts of carbonaceous products were formed.

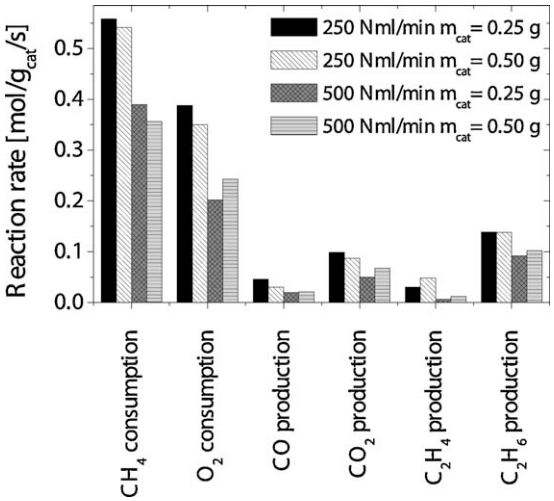


**Fig. 4.** Reaction rates at different flow rates ($p_{o_2}$ = 8 kPa, $p_{CH_4}$ = 50 kPa, $T$ = 800 °C, $p$ = 200 kPa, $\phi_v$ = 250–500 Nml/min, $m_{cat}$ = 0.25–0.50 g).

With quartz as a reactor material, it is shown that conversion of $CH_4$ and $O_2$ takes place significantly, especially at higher temperatures (see Fig. 5). For accurate determination of the reaction kinetics it is however necessary to minimize the influence of gas phase reactions as much as possible, which was realized by reduction of the void space by filling the pre- and post-catalytic volume with inert quartz particles (1–2 mm). It can be seen that the reaction rates have decreased with a factor 5, so that the $O_2$ conversion is less than 3%, which is an acceptable level for measuring the reaction rates at 800 °C.

### 2.3.5. Experimental procedure

For the kinetic measurements, the post- and pre-catalytic reactor volume was filled with quartz chips of 1–2 mm and a catalyst mass up to 0.5 g was used. The reactor inlet and outlet temperature was measured with two K-type thermocouples.

Prior to the experiments, the setup was tested for leaks with $N_2$ at an operating pressure of 2 bar, first at room temperature and then at process temperature. First, the homogeneous gas phase reactions were measured at 800 °C and 2 bar, with different mixtures of $CH_4$, air and $N_2$ at a total flow rate of 250 ml/min. Subsequently, the reactor was filled with the $Mn/Na_2WO_4/SiO_2$ catalyst (max. 0.5 g, $d_p$ = 0.5 mm) and heated until process temperature with a ramp rate of 5–10 °C/min under a flow of air to ensure the catalyst is in the oxidized state.

Before starting the kinetic measurements, the reactor was purged with $N_2$ for at least 10 min to ensure all air has been removed. The feed composition for each test was measured with the flow by-passing the reactor (see Fig. 2). After the flow was switched to the reactor, the outlet composition was measured on the GC and process parameters were logged.

It was shown that the gas-phase reactions cannot be completely prevented from occurring in pre- and post-catalytic zone during experiments with catalyst. To get insight into solely the

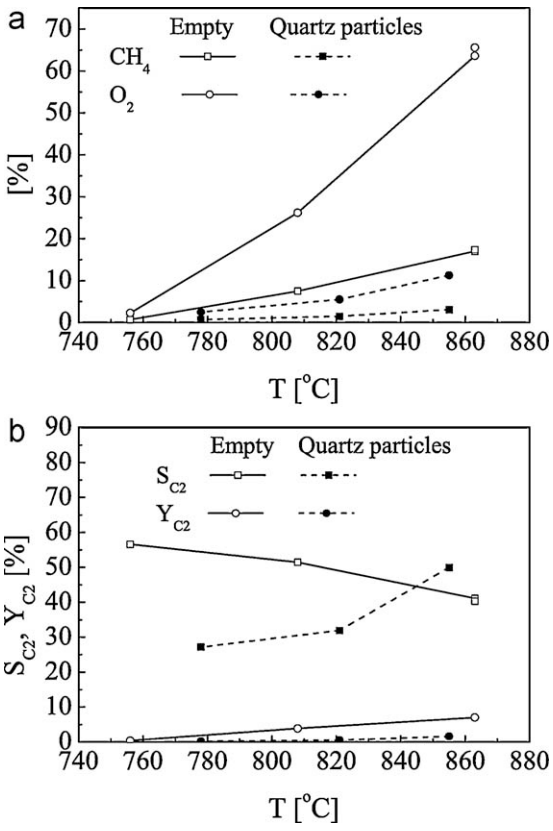


**Fig. 5.** Extent of gas phase reactions at different temperatures in an empty tube and in a reactor filled with quartz particles ($d_p$ = 1 − 2 mm) on (a) conversion and (b) selectivity and yield ($CH_4/O_2/N_2$ = 4:1:4, $\phi_v$ = 250 Nml/min, $p$ = 200 kPa).

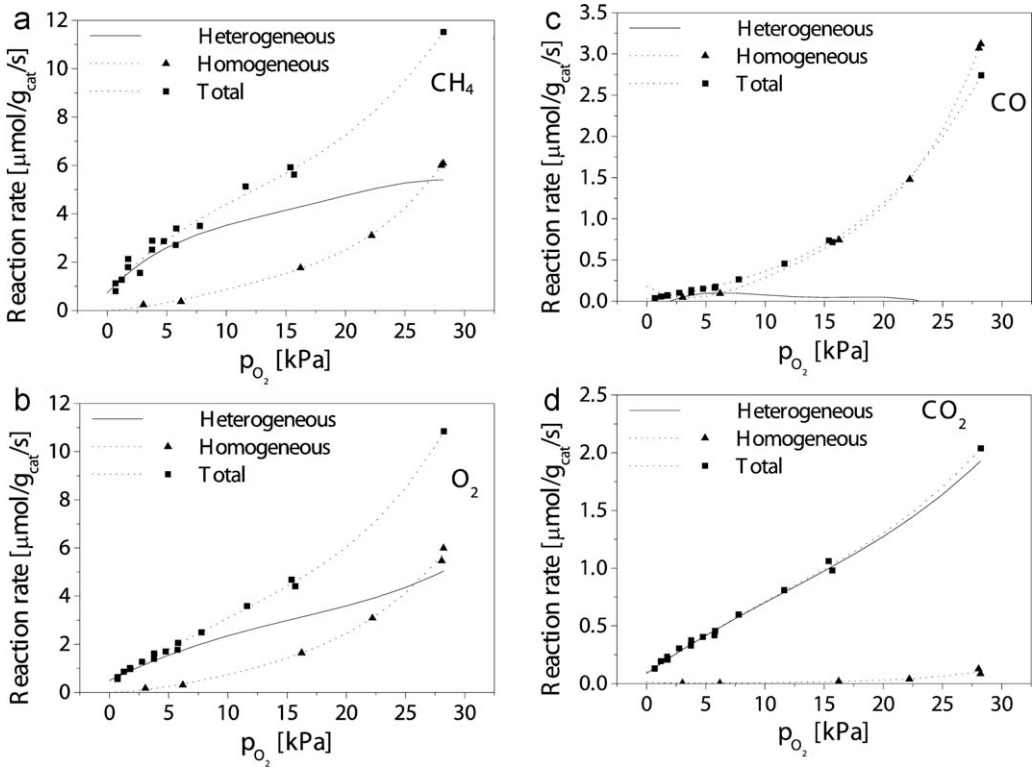


**Fig. 6.** Influence of the $p_{O2}$ on the $CH_4$ and $O_2$ consumption rates and the CO and $CO_2$ production rates ($p_{CH_4}$ = 50 kPa, $T$ = 800 °C and $p$ = 200 kPa, $m_{cat}$ = 0.25 g, $\phi_v$ = 250 Nml/min).

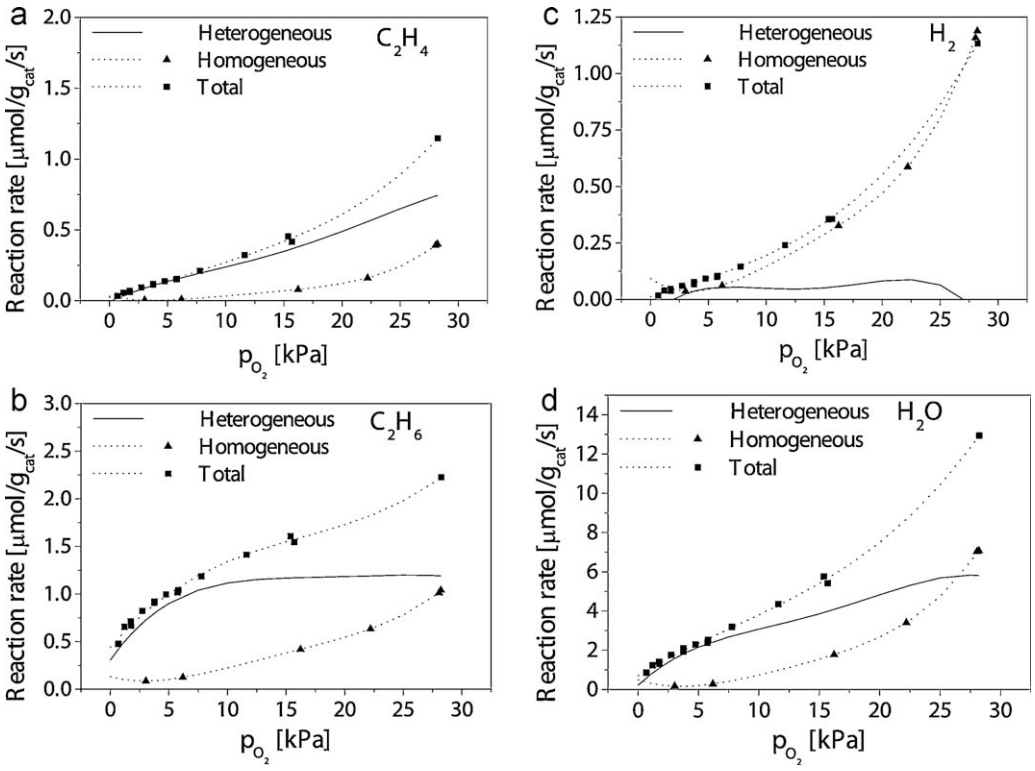


**Fig. 7.** Influence of the $p_{o_2}$ on the $C_2H_4$, $C_2H_6$, $H_2$ and $H_2O$ production rates ($p_{CH_4}$ = 50 kPa, $T$ = 800 °C and $p$ = 200 kPa, $m_{cat}$ = 0.25 g, $\phi_v$ = 250 Nml/min).

heterogeneous reactions, the rates measured during experiments without catalyst present are subtracted from the rates from experiments with catalyst, assuming there is no interaction between heterogeneous and gas-phase reactions.

Because the rates are not exactly obtained at the same partial pressures, the experimental results are fitted, with linear, power law or polynomial trends and subsequently the catalytic contribution is calculated.

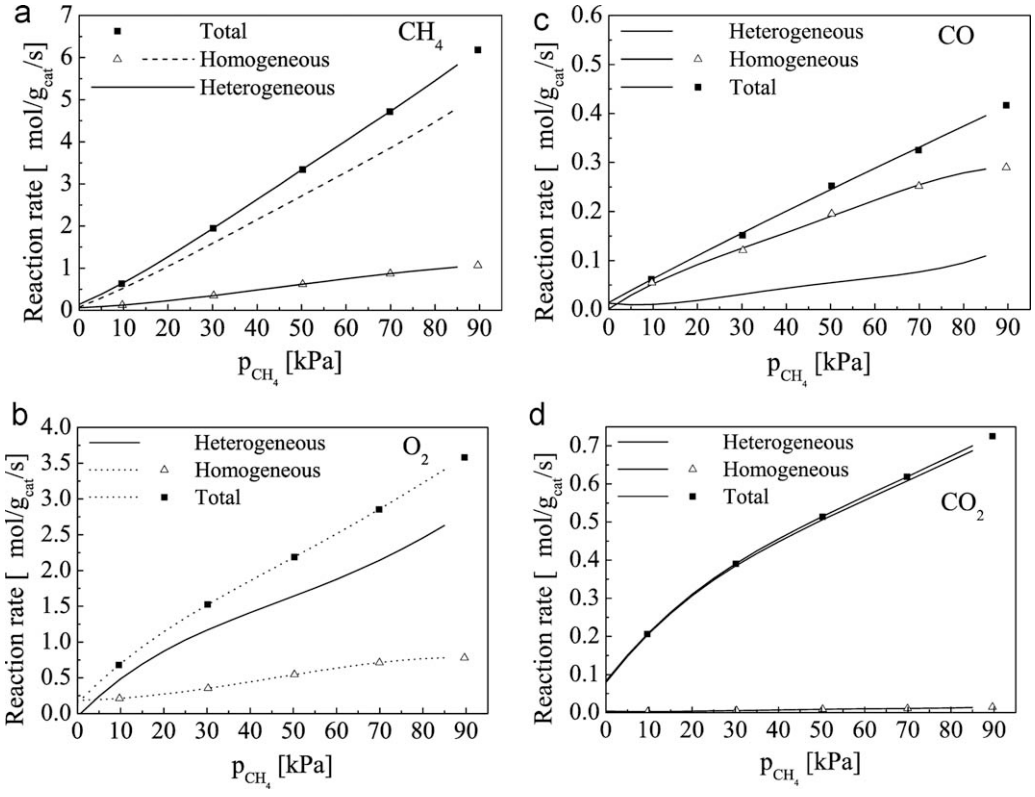


**Fig. 8.** Influence of the $p_{CH4}$ the $CH_4$ and $O_2$ consumption rates and the CO and $CO_2$ production rates ($p_{o_2}$ = 8 kPa, $T$ = 800 °C and $p$ = 200 kPa, $m_{cat}$ = 0.25 g, $\phi_v$ = 250 Nml/min).

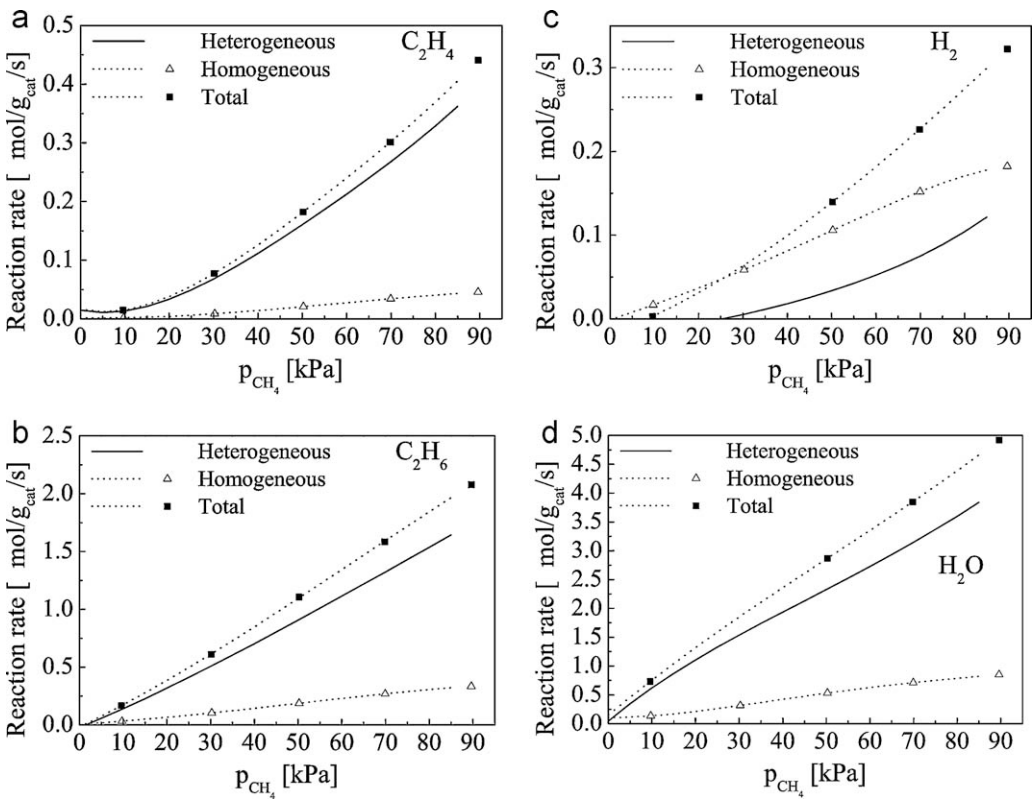


**Fig. 9.** Influence of the $p_{CH_4}$ on the $C_2H_4$, $C_2H_6$, $H_2$ and $H_2O$ production rates ($p_{O_2}$ = 8 kPa, $T$ = 800 °C and $p$ = 200 kPa, $m_{cat}$ = 0.25 g, $\phi_v$ = 250 Nml/min).

## 3. Results

The kinetic measurements have been carried out at a constant temperature of 800 °C and a pressure of 2 bar. Different $CH_4$ and $O_2$ inlet concentrations were applied, to investigate the influence of the concentrations on the intrinsic reaction rate and to determine the reaction orders. Differential operating conditions were used, so that the overall $O_2$ conversion was always below 25% and the $CH_4$ conversion below 6.5%.

### 3.1. Primary reaction rates

The primary reaction rates were measured under differential conditions, first to determine the contribution of homogeneous gas phase reactions (also in the pre- and post catalytic sections) using the reactor filled with only quartz particles and subsequently for the reactor filled with the $Mn/Na_2WO_4/SiO_2$ catalyst.

In Figs. 6 and 7, the influence of the $O_2$ partial pressure on the gas phase and the total reaction rates are plotted. The calculated heterogeneous contribution (substracting the gas phase reaction rate from the total measured reaction rate) is also displayed.

Comparing the extent of gas phase reactions to the total reaction rate, it can be concluded that at low $O_2$ partial pressures, the most interesting concentration range for OCM, there is hardly any influence of gas phase reactions on the total reaction rate and the $C_2$ selectivity is high (Figs. 6 and 7). Above an oxygen partial pressure of 10 kPa, however, it can be seen that particularly carbon monoxide and hydrogen are almost entirely generated in the gas phase, while $CO_2$ is only produced in small amounts over the entire range of $O_2$ partial pressures investigated. It can be concluded that the contribution of the catalyst to $H_2$ and CO production is negligible.

Ethane is only formed in the gas phase at $p_{O2}$ higher than 7–10 kPa due to coupling reactions, while $C_2H_4$ can be considered as a secondary product which will only be generated in sufficient amounts at higher $CH_4$ conversions. The catalyst clearly leads to selective $C_2H_6$ formation, already at low $O_2$ pressures, but the net generation rate is decreasing at higher $O_2$ pressures because a part of $C_2H_6$ is likely to be dehydrogenated to $C_2H_4$.

It can be seen that the overall reaction order for each component is slightly different in the gas phase, particularly for the CO formation rate the $O_2$ reaction order is rather high, while the other components show reaction orders in $O_2$ slightly higher than 1, which results in a decreasing $C_2$ selectivity at higher $O_2$ concentrations.

A second set of experiments was performed, but in this series a constant $O_2$ partial pressure of 8 kPa was used while the $CH_4$ inlet partial pressure was varied. From Figs. 8 and 9 it can be inferred that nearly all components show first order dependency on the $CH_4$ concentration. Products of the gas phase reactions are mainly CO and $C_2H_6$, as also observed before in the experiments when varying the $O_2$ concentration. At higher $CH_4$ partial pressures, it seems that the catalytic partial oxidation to CO and $H_2$ is gaining some importance, as can be inferred from the increasing catalytic contribution to CO production (Fig. 10)

The contribution is however still small, as the catalytic production rate of $C_2H_6$ is much higher. The large difference between $C_2H_6$ and $C_2H_4$ generation rates (note the different scales in Fig. 9a and b) again confirms that $C_2H_4$ can be considered as mostly a secondary product.

### 3.2. Kinetic model

The derivation of the kinetic model is also split into two parts. During the measurements at differential conditions, the secondary

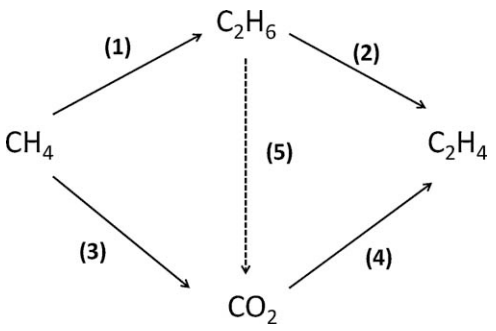


**Fig. 10.** Schematic simplified reaction scheme for the oxidative coupling of methane on $Mn/Na_2WO_4/SiO_2$.

reaction rates can be neglected and the reaction rate constants of the primary reactions can directly be determined. The kinetic model for the primary reactions then serves as a basis for the calculation of the secondary reaction rate constants from the literature.

*3.2.1. Assumptions*

The measurements at various $CH_4$ and $O_2$ inlet concentrations at differential operating conditions have led to experimental data which can be used to derive a simplified kinetic model. The following preliminary conclusions can be made:

- The oxidation reaction to CO proceeds mainly in the gas phase.
- The origin of $CO_2$ is mainly $CH_4$ at the used differential conditions.
- The oxidative coupling reaction produces the primary reaction product $C_2H_6$.
- Ethylene is mainly generated via $C_2H_6$ oxidative dehydrogenation.
- The secondary oxidation reactions can be neglected at the used conditions.

These observations will be shortly discussed in the following sections.

*3.2.2. (Oxidative) dehydrogenation of ethane*

Two pathways exist for $C_2H_4$ formation, the oxidative (reaction (5)) and the thermal (reaction (6)) dehydrogenation reaction. Experiments with a feed of 50 kPa $C_2H_6$ without and with 1 kPa $O_2$ have been carried out in a reactor with 0.25 g of catalyst at 800 °C at 200 kPa to examine the relative rates of these reactions. The experiment with $O_2$ showed 50% $C_2H_6$ conversion and almost 100% conversion of $O_2$. Most $C_2H_6$ is converted to $C_2H_4$ (selectivity 98.6%) and all $O_2$ reacted to $CO_2$.

Also traces of $CH_4$ were found in the product stream, but this reaction is neglected due to the low significance. The experiment without $O_2$ showed similar $C_2H_6$ conversion and $C_2H_4$ formation and the temperature inside the reactor dropped slightly when the mixture was fed to the reactor, indicating that the endothermic thermal dehydrogenation reaction took place and not the exothermic oxidative dehydrogenation.

At higher $O_2$ concentrations, however, it is expected that the oxidative dehydrogenation has a more important contribution; therefore the reaction will be incorporated in the kinetic model.

*3.2.3. Hydrogen oxidation*

Partial oxidation of $CH_4$ and $C_2$ and the dehydrogenation of $C_2H_6$ lead to $H_2$ formation. It is likely that $H_2$ will react fast with $O_2$ to form water (reaction (13)). Several studies on the reaction mechanism of $H_2$ oxidation have been reported in the literature [38,39] and it is believed that it consists of 19 elementary steps. The behavior is complex, as the reaction rates are dependent of three explosion limits. The exact location of the explosion limits depends on various factors such as the size of the reaction vessel, the surface-to-volume ratio, and the initial reactant concentrations (including inert components, such as $N_2$ etc.) [40].

Impurities and the reactor surface (even quartz) will influence reaction rates, so that it is difficult to determine the reaction rates of $H_2$ oxidation at OCM conditions. Furthermore there is no information in the literature whether $Mn/Na_2WO_4/SiO_2$ will catalyze this reaction. The experimental results show that $H_2$ formation in the presence of this catalyst is similar to that in the gas-phase. At first sight it might be concluded that the catalyst has no influence on hydrogen oxidation. However, in the presence of the catalyst much higher $C_2H_4$ reaction rates are measured, which are formed by dehydrogenation of ethane. The accompanied $H_2$ production is not measured at the reactor outlet.

Additional difficulty is that most dehydrogenation will take place in the post-catalytic zone. The most probable explanation for the observed results is that the hydrogen produced during gas-phase partial oxidation of $CH_4$ in the pre-catalytic zone is (partly) catalytically oxidized to water, followed by $H_2$ production in the post-catalytic zone by dehydrogenation. This might be the reason why the net hydrogen production is similar for experiments with and without catalyst. To enhance the understanding of the later proposed mechanism, it is assumed that all $H_2$ formed during catalyzed reactions and the dehydrogenation of ethane is converted to water.

*3.2.4. Ethane and ethylene oxidation*

To get insight into the primary and secondary reactions of OCM, it is important to know the origin of the unselective products CO and $CO_2$. Next to CO being a primary and secondary oxidation product, it has been reported that good coupling catalysts generally are also effective for the conversion of CO to $CO_2$ [36].

Thus, although the catalytic contribution to CO formation seems negligible, it might be produced much faster in the experiments with a catalyst, but is converted at a similar rate in a consecutive reaction to $CO_2$ (reactions (11) and (12)). However, here it is assumed that the $CH_4$ conversion to CO is not catalyzed. Experimental verification of the origin of the carbon oxides, was carried out with $C_2H_6$ in the feed at an $O_2$ partial pressure of 15 kPa. The inlet concentration of 0.5 kPa $C_2H_6$ was based on the average concentration measured in the reactor outlet during differential measurements of OCM. Surprisingly, in experiments without and with 0.25 g catalyst, in both cases it was found that $C_2H_6$ is totally converted and CO and $CO_2$ are formed at $1.86 \times 10^{-6}$ and $2.05 \times 10^{-6}$ mol/(g s) respectively, which is higher than the measured rates at the experiments with only $CH_4$ and $O_2$ in the feed (Figs. 6 and 7).

The results can be explained by considering the fact that if $CH_4$ is not present in the feed streams, which has been reported to have an inhibiting effect on $C_2H_6$ and $C_2H_4$ oxidation in the gas phase [25,30].

It was also attempted to determine the $C_2$ secondary oxidation reaction rates in the micro-catalytic reactor by co-feeding $C_2H_4$ or $C_2H_6$ at different $O_2$ and $CH_4$ inlet concentrations, however, this resulted in an unacceptable error in the carbon mole balance and differential conditions could not be obtained ($C_2H_6$ conversion of more than 40%). In addition, a significant deviation from isothermal operation was observed because of the strongly exothermic reactions. Furthermore, it cannot be excluded that part (or all) of the $C_2$ products are already converted prior to reaching the catalyst bed in the pre-catalytic zone, which inevitably results in large inaccuracies in the determination of the kinetic parameters of secondary reactions.

Because the secondary oxidation reactions of $C_2H_4$ and $C_2H_6$ could not be measured and the source of $CO_x$ could not be

elucidated, the influence of $C_2H_4$ and $C_2H_6$ oxidation was estimated by comparing the obtained experimental results with the reaction rate constants determined by Takanabe and Iglesia [4]. They recently measured the first order rate constants on a $Mn/Na_2WO_4/SiO_2$ catalyst in a recirculating batch reactor at differential operating conditions. Isotopic labeling of $CH_4$, $C_2H_4$ and $C_2H_6$ allowed for accurate determination of the rate constants, unraveling the complex catalyzed reactions in the OCM process, which was also performed by other researchers [4,25,36].

It was found that the contribution of secondary oxidation of $C_2$ components to carbon oxides depends on many parameters, and it appears that the rate constant for $CO_2$ formation from $C_2H_4$ is 68 times larger than that for $CH_4$ oxidation, while $C_2H_6$ combustion plays no significant role [25]. Takanabe and Iglesia [4] found a ratio between the reaction rate constant of $C_2H_4$ and $CH_4$ oxidation of 4.3, which confirms the measurements of Pak and Lunsford [25]. In contrary to other researchers, they also found that the ratio between $C_2H_6$ and $CH_4$ oxidation is 2.7, which suggests that $C_2H_6$ oxidation cannot be neglected in the kinetic model if it is kept in mind that typically the $C_2H_6$ concentration is much larger than that of $C_2H_4$, particularly at higher $CH_4$ concentrations (see also Fig. 9a and b). At the differential conditions used in the experiments, however, the total contribution of $C_2H_4$ and $C_2H_6$ to $CO_2$ formation is in general lower than from $CH_4$ oxidation, because $CH_4$ conversion is typically lower than about 30–50% because of the desired high $CH_4/O_2$ ratios. Therefore, it can be assumed that the contribution of $C_2H_4$ and $C_2H_6$ oxidation to the $CO_2$ formation rate can be mostly neglected for the derivation of the primary reaction rate constants.

Furthermore, it is assumed that CO formed on the catalyst surface is immediately converted to $CO_2$, which probably is a catalyzed reaction as described above. To simplify the mechanism further, it is assumed that CO formed in the gas phase will not react on the catalyst to $CO_2$.

## 4. Discussion

### 4.1. Proposed simplified mechanism

Based on the analysis of the obtained experimental results and relevant publications in the literature, the next simplified reaction mechanism for the heterogeneous reaction rates (corrected for gas-phase reactions) is proposed:

Because no inhibition effects have been identified, the rates will be represented by simple power-law or linear relations. Only the total conversion rates were derived from the experimental results, and the reaction rates of the individual reactions (1–5) were calculated based on the reaction stoichiometry and the assumptions that CO and $H_2$ are not generated catalytically and that there is no interaction with gas phase reactions. Because the gas phase reactions in the post-catalytic zone will be influenced by the higher concentrations of the reaction products ($C_2H_6$), there will be some additional dehydrogenation and oxidation reactions, but here it is assumed that the influence on the overall reaction rate is low.

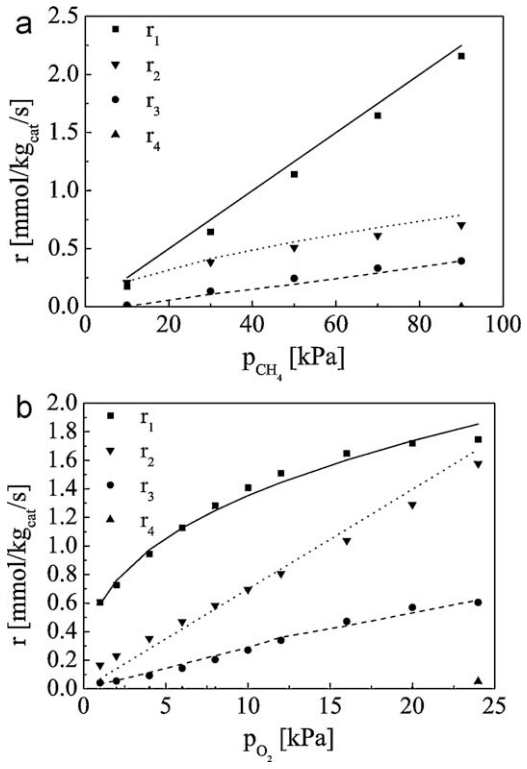


**Fig. 11.** Comparison of the kinetic model fit with the measured reaction rates (a) $CH_4$ partial pressure and (b) $O_2$ partial pressure.

The result of the calculated reaction rates from the experimental data for the individual reactions in the proposed reaction scheme is displayed in Fig. 11a and b (markers).

Clearly, the secondary oxidation of $C_2H_4$ (reaction (4)) can be neglected, because the calculated reaction rate of this reaction is much lower than the other reactions at differential conditions, as was concluded earlier. Hence, for the determination of the reaction rate constants and reaction orders, only reactions (1–3) have been taken into account. The kinetic parameters were evaluated, by fitting the calculated reaction rates to the suggested power-law rate expression (Table 5), based on least squares minimization:

$$\varepsilon = \sum^{\text{datapoints}} \left( \frac{r_{\text{measured}} - r_{\text{fit}}}{r_{\text{measured}}} \right)^2$$

As shown in Fig. 11a and b, it can be seen that the fitted reaction rates are in quite reasonable agreement with the rates actually observed and therefore it can be concluded that the proposed mechanism is describing the experimental results adequately.

The results of the error minimization are summarized in Table 5. Reactions (4) and (5) were omitted in the minimization, because of the negligible reaction rates in these experiments. However, assuming first order in $O_2$, $C_2H_6$ and $C_2H_4$, the reaction rate con-

**Table 5**
Kinetic parameters obtained via the least squares minimization of the OCM experiments at differential conditions (with $k_i$ in mmol/kg/s/kPa$^{mi+ni}$).

| $i$ | Reaction | Expression | $k_i$ | $n_i$ | $m_i$ |
|---|---|---|---|---|---|
| | *Based on measurements* | | | | |
| (1) | $2CH_4 + ½O_2 \rightarrow C_2H_6 + H_2O$ | $r_1 = k_1 p_{CH_4}^{n_1} p_{O_2}^{m_1}$ | 0.0118 | 1.0 | 0.36 |
| (2) | $CH_4 + 2O_2 \rightarrow CO_2 + 2H_2O$ | $r_2 = k_2 p_{CH_4}^{n_2} p_{O_2}^{m_2}$ | 0.00702 | 0.59 | 1.0 |
| (3) | $C_2H_6 + ½O_2 \rightarrow C_2H_4 + H_2O$ | $r_3 = k_3 p_{C_2H_6}^{n_3} p_{O_2}^{m_3}$ | 0.2008 | 1.0 | 0.58 |
| | *Based on (Takanabe and Iglesia (2008))* | | | | |
| (4) | $C_2H_4 + 3O_2 \rightarrow 2CO_2 + 2H_2O$ | $r_4 = k_4 p_{C_2H_4}^{n_4} p_{O_2}^{m_4}$ | 0.0520 | 1.0 | 1.0 |
| (5) | $C_2H_6 + 7/2O_2 \rightarrow 2CO_2 + 3H_2O$ | $r_5 = k_5 p_{C_2H_6}^{n_5} p_{O_2}^{m_5}$ | 0.0331 | 1.0 | 1.0 |

stants can be roughly estimated if the ratio $k_4/k_1$ is equal to 4.3 and $k_5/k_1$ equal to 2.7, which is based on the data published by Takanabe and Iglesia [4].

Based on the experimental results in Fig. 11a and b, it was assumed that the reaction orders in $CH_4$ for reactions (1) and (3), and the $O_2$ reaction order of reaction (3) were equal to 1.0. This result is well in agreement with earlier obtained results from e.g. [8] on a different catalyst.

The reaction order of 1.0 for $O_2$ for reaction (2) was also observed by Stansch. Clearly, it can be seen that while reactions (1) and (3) have a reaction order of approximately 1.0 to the hydrocarbons, a lower reaction order in $CH_4$ was found for the methane oxidation (reaction (2)), which is also observed by Stansch [8]. An important result is that the reaction order in $O_2$ for the coupling and dehydrogenation reaction is lower than unity, while the reaction in methane combustion is equal to one, which results in a higher $C_2$ selectivity at lower $O_2$ partial pressures.

Over the entire range of reactants pressures it is observed that the primary OCM reaction rates can be predicted well by the developed power-law reaction rate equations.

## 5. Conclusions

In this work, the performance of the $Mn/Na_2WO_4/SiO_2$ for oxidative coupling of methane was investigated because it was found that this catalyst has excellent long-term stability and moderate catalytic activity.

The objective was to characterize the behavior of the catalyst and to obtain a kinetic model which can describe the reaction rates with sufficient accuracy for reactor modeling studies. First, the catalyst was prepared and experiments in a micro-catalytic fixed bed reactor under integral conditions have confirmed that $C_{2+}$ yields of more than 20% can be obtained in the oxidative coupling of methane using a $Mn/Na_2WO_4/SiO_2$ catalyst at 830 °C, which is in agreement with results reported in literature.

By means of Thermal Gravity Analysis (TGA) it was determined that the catalyst, which is a reducible metal oxide, requires pretreatment with oxygen/air to obtain a high $C_2$ selectivity and stable reactor performance. The intrinsic catalytic reaction rates were calculated from the measured reaction rates with and without catalyst at differential operating conditions. At a $CH_4$ partial pressure in the range of 1090 kPa and a $O_2$ partial pressure in the range of 0.730 kPa at 800 °C and 200 kPa, the reaction rates for the reactions (oxidative coupling, total oxidation of $CH_4$ and oxidative dehydrogenation of $C_2H_6$) were derived from the experimental data and fitted with power-law reaction rate expressions.

It was found that $C_2H_6$ formation is linearly dependent on the $CH_4$ concentration, while the dependency on the $O_2$ partial pressure can be described by a power law function with a reaction order in $O_2$ of 0.36, confirming observations of other researchers. At differential operating conditions, the secondary $C_2H_4$ reaction rates could not be determined, however, reaction rates can be well described with data available in the literature, in which it was found that the reaction rate of $C_2H_4$ oxidation is 2–8 times larger than for $CH_4$ oxidation. These results signify that highest $C_2$ selectivities can be obtained at high $CH_4$ and low $O_2$ partial pressures, best achieved in reactor systems with distributed oxygen feed.

## Acknowledgement

The authors would like to acknowledge the financial support by the Netherlands Organisation for Scientific Research (NWO/ACTS) under the research theme of Advanced Sustainable Processes by Engaging Catalytic Technologies (ASPECT) (project 053.62.008).

## References

[1] G.E. Keller, M.M. Bhasin, J. Catal. 73 (1982) 9–19.
[2] T. Ito, J. Wang, C. Lin, J.H. Lunsford, J. Am. Chem. Soc. 107 (1985) 5062–5068.
[3] S.J. Korf, J.A. Roos, L.J. Veltman, J.G. van Ommen, J.R.H. Ross, Appl. Catal. 56 (1989) 119–135.
[4] K. Takanabe, E. Iglesia, Angew. Chem. Int. Ed. 47 (2008) 7689–7693.
[5] V.R. Choudhary, B.S. Uphade, Catal. Surveys Asia 8 (2004) 15–25.
[6] S. Kus, M. Otremba, M. Taniewski, Fuel 82 (2003) 1331–1338.
[7] A.G. Dedov, A.S. Loktev, I.I. Moiseev, A. Aboukais, J.F. Lamonier, I.N. Filimonov, Appl. Catal. A: Gen. 245 (2003) 209–220.
[8] Z. Stansch, L. Mleczko, M. Baerns, Ind. Eng. Chem. Res. 36 (1997) 2568–2579.
[9] S.J. Conway, J.A. Greig, G.M. Thomas, Appl. Catal. A: Gen. 86 (1992) 199–212.
[10] J.M. DeBoy, R.F. Hicks, Ind. Eng. Chem. Res. 27 (1988) 1577–1582.
[11] J. Wang, L. Chou, B. Zhang, H. Song, J. Zhao, J. Yang, S. Li, J. Mol. Catal. A: Chem. 245 (2006) 272–277.
[12] A. Palermo, J.P.H. Vazquez, A.F. Lee, M.S. Tikhov, R.M. Lambert, J. Catal. 177 (1998) 259–266.
[13] S. Ji, T.-c. Xiao, S.-b. Li, C.-z. Xu, R.-l. Hou, K.S. Coleman, M.L.H. Green, Appl. Catal. A: Gen. 225 (2002) 271–284.
[14] L. Chou, Y. Cai, B. Zhang, J. Niu, S. Ji, S. Li, Appl. Catal. A: Gen. 238 (2003) 185–191.
[15] S. Pak, P. Qiu, J.H. Lunsford, J. Catal. 179 (1998) 222–230.
[16] Z.C. Jiang, C.J. Yu, X.P. Fang, S.B. Li, H.L. Wang, J. Phys. Chem. 97 (1993) 12870–12875.
[17] S. Becker, M. Baerns, J. Catal. 128 (1991) 512–519.
[18] J. Lunsford, Catal. Today 6 (1990) 235–259.
[19] J. Lunsford, Catal. Today 63 (2000) 165–174.
[20] X. Fang, S. Li, J. Gu, D. Yang, J. Mol. Catal. (China) 6 (1992) 427–433.
[21] J.A. Sofranko, J.J. Leonard, C.A. Jones, J. Catal. 103 (1987) 302–310.
[22] C.A. Jones, J.J. Leonard, J.A. Sofranko, J. Catal. 103 (1987) 311–319.
[23] J.A. Sofranko, J.J. Leonard, C.A. Jones, A.M. Gaffney, H.P. Withers, Catal. Today 3 (1988) 127–135.
[24] D.J. Wang, M.P. Rosynek, J.H. Lunsford, J. Catal. 155 (1995) 390–402.
[25] S. Pak, J.H. Lunsford, Appl. Catal. A: Gen. 168 (1998) 131–137.
[26] Y. Kou, B. Zhang, J. Niu, S. Li, H. Wang, T. Tanaka, S. Yoshida, J. Catal. 173 (1998) 399–408.
[27] S. Ji, T. Xiao, S. Li, L. Chou, B. Zhang, C. Xu, R. Hou, A.P.E. York, M.L.H. Green, J. Catal. 220 (2003) 47–56.
[28] H. Zhang, J. Wu, B. Xu, C. Hu, Catal. Lett. 106 (2006) 161–165.
[29] P.M. Couwenberg, Q. Chen, G.B. Marin, Ind. Eng. Chem. Res. 35 (1996) 415–421.
[30] J.A. Roos, S.J. Korf, R.H.J. Veehof, J.G. van Ommen, J.R.H. Ross, Appl. Catal. 52 (1989) 131–145.
[31] G.C. Hoogendam, The oxidative coupling of methane over doped Li/MgO catalysts, PhD thesis, (1996) University of Twente.
[32] G.A. Martin, C. Mirodatos, Fuel Process. Technol. 42 (1995) 179–215.
[33] Q. Chen, P.M. Couwenberg, G.B. Marin, Catal. Today 21 (1994) 309–319.
[34] P.M. Couwenberg, Gas-phase chain reactions catalyzed by solids: the oxidative coupling of methane, PhD thesis, (1995) Eindhoven University.
[35] P.F. Nelson, N.W. Cant, J. Phys. Chem. 94 (1990) 3756–3761.
[36] C. Shi, M.P. Rosynek, J.H. Lunsford, J. Phys. Chem. 98 (1994) 8371–8376.
[37] A. Ekstrom, R. Regtop, S. Bhargava, Appl. Catal. 62 (1990) 253–269.
[38] M. O'Conaire, H.J. Curran, J. Simmie, W.J. Pitz, C.K. Westbrook, Int. J. Chem. Kinet. 36 (2004) 603–622.
[39] M.A. Mueller, T.J. Kim, R.A. Yetter, F.L. Dryer, Int. J. Chem. Kinet. 31 (1999) 113–125.
[40] G. Veser, Chem. Eng. Sci. 56 (2001) 1265–1273.
[41] D.E. Mears, J. Catal. 20 (1971) 127–131.
[42] D.E. Mears, Ind. Eng. Chem. Process Des. Dev. 10 (1971) 541–547.